

NMR spin-echo spectra of icosahedral quasicrystals

W. W. Warren, Jr., H. S. Chen, and J. J. Hauser

AT&T Bell Laboratories, Murray Hill, New Jersey 07974

(Received 16 August 1985)

We report ^{27}Al and ^{55}Mn spin-echo spectra for the icosahedral quasicrystals $\text{Al}_{86}\text{Mn}_{14}$ and $\text{Al}_{72}\text{Si}_6\text{Mn}_{22}$ and for the amorphous and equilibrium crystalline forms of $\text{Al}_{86}\text{Mn}_{14}$. The distribution of local electric-field-gradient magnitudes at the Al sites in icosahedral $\text{Al}_{86}\text{Mn}_{14}$ is only slightly narrower than in the amorphous form, but the local asymmetry in the former is significantly restricted to lower values. A corresponding degree of order is not detectable for the Mn sites in icosahedral $\text{Al}_{86}\text{Mn}_{14}$ for which the distribution of the local environments is comparable with that observed in amorphous material. Broad distributions are also inferred for both Al and Mn sites in icosahedral $\text{Al}_{72}\text{Si}_6\text{Mn}_{22}$.

The recent observation¹ of sharp Bragg diffraction patterns with fivefold rotational symmetry has drawn broad attention to rapidly quenched Al-transition-metal alloys. Long-range orientational order with icosahedral point symmetry has been found in $\text{Al}_{86}\text{Mn}_{14}$ and analogues in which Fe or Cr replaces Mn. A superlattice structure of icosahedral symmetry was recently reported² for ternary systems of the type $\text{Al}_{94-x}\text{Si}_6\text{Mn}_x$ with x in the range 20–22 at.%. The unusual structures of these so-called “quasicrystals” are of considerable intrinsic interest and, moreover, are important for the insight they may provide into the structure of amorphous metals.³ However, the details of the quasicrystal structures remain poorly understood. While it has been shown^{4–6} that mathematical models based on three-dimensional Penrose tilings reproduce the diffraction patterns quite accurately, little is known of the actual atomic positions in the alloys.

In this Rapid Communication we report the first nuclear magnetic resonance (NMR) results for quasicrystalline alloys. The sensitivity of NMR to the local environment, particularly the local electric-field-gradient (EFG) tensor, and the possibility of discriminating among the chemical species (e.g., Al and Mn) permit determination of some basic characteristics of the local atomic arrangements. The similarity of a number of properties to those of amorphous material^{7–9} suggests that icosahedral $\text{Al}_{86}\text{Mn}_{14}$ consists of a highly disordered structure. We have therefore given special attention to examining the differences between the icosahedral and amorphous forms.

We report ^{27}Al and ^{55}Mn spin-echo spectra for three structural forms of $\text{Al}_{86}\text{Mn}_{14}$: the icosahedral quasicrystal ($\text{Al}_{86}\text{Mn}_{14}\text{-I}$), the crystalline equilibrium state which is predominately orthorhombic Al_6Mn ($\text{Al}_{86}\text{Mn}_{14}\text{-O}$), and the amorphous form ($\text{Al}_{86}\text{Mn}_{14}\text{-a}$). We also report data for a ternary quasicrystal, $\text{Al}_{72}\text{Si}_6\text{Mn}_{22}\text{-I}$. The results show that there is sufficient order in the distribution of EFG parameters at the Al sites in $\text{Al}_{86}\text{Mn}_{14}\text{-I}$ to preserve some spectral features of a polycrystalline quadrupole splitting. This permits rough estimates to be made of the range of local EFG values and local asymmetry in the quasicrystal and of the relative degrees of order in these parameters in the icosahedral and amorphous forms. No corresponding difference in order could be detected for the Mn sites in the two forms; nor could quadrupole splittings be resolved in $\text{Al}_{72}\text{Si}_6\text{Mn}_{22}$.

Quasicrystal samples were prepared by spin quenching to

yield material in ribbon form roughly 1 mm wide by 30 μm thick. The samples were examined by transmission electron microscopy and were found to exhibit the typical icosahedral diffraction pattern. To obtain the equilibrium phase $\text{Al}_{86}\text{Mn}_{14}\text{-O}$, we annealed the ribbon with this composition for 20 h at 550°C. Amorphous $\text{Al}_{86}\text{Mn}_{14}$ was sputtered from the corresponding induction-melted alloy onto a NaCl substrate, which was subsequently dissolved away to yield a free standing film of 30–40- μm thickness. The NMR samples had weights in the range 50–100 mg and were prepared in powder form by crushing the brittle films or ribbons in an agate mortar.

Field-swept spin-echo spectra at 4.2 K were obtained at various fixed frequencies in the range 10.4–18.3 MHz. We made measurements at more than one frequency as an aid to separating the overlapping ^{27}Al and ^{55}Mn spectra. To improve the signal-to-noise ratio for the small samples, it was necessary to collect data from repeated field sweeps in a signal averager.

In Fig. 1 we present representative spin-echo spectra for the three forms of $\text{Al}_{86}\text{Mn}_{14}$ and $\text{Al}_{72}\text{Si}_6\text{Mn}_{22}\text{-I}$. A general feature of all spectra is a relatively narrow central peak associated with the ^{27}Al $m = \pm \frac{1}{2}$ transition superimposed on a broad spectrum due to electric quadrupole splitting. All samples also exhibited a weak, narrow resonance due to rejected, second-phase aluminum. This “pure Al” line does not contribute to the spin-echo spectra shown in Fig. 1 and was detected most readily by its free-induction-decay signal following a single radio frequency pulse.

A narrow ^{55}Mn central peak appears only in the spectrum of $\text{Al}_{86}\text{Mn}_{14}\text{-O}$ [Fig. 1(a)]. In the amorphous and icosahedral phases [Figs. 1(b) and 1(c)], it is replaced by a broad line having no discernible structure. The ^{55}Mn peak is not resolved for $\text{Al}_{72}\text{Si}_6\text{Mn}_{22}$ at these frequencies [Fig. 1(d)], but the resonance is revealed by a broad asymmetry in the overall spectrum.

A more detailed comparison of the broad spectra of the icosahedral and amorphous forms of $\text{Al}_{86}\text{Mn}_{14}$ is shown in vertical expansion in Fig. 2. The essential difference is the presence in the spectrum for $\text{Al}_{86}\text{Mn}_{14}\text{-I}$ of a pronounced shoulder on the low-field side of the main peak. This feature is completely absent for the amorphous sample even though the overall widths of the spectra are comparable for the two cases. Careful comparisons at different frequencies showed that the low-field shoulder remains at a fixed separation from the narrow ^{27}Al line as expected for a first-

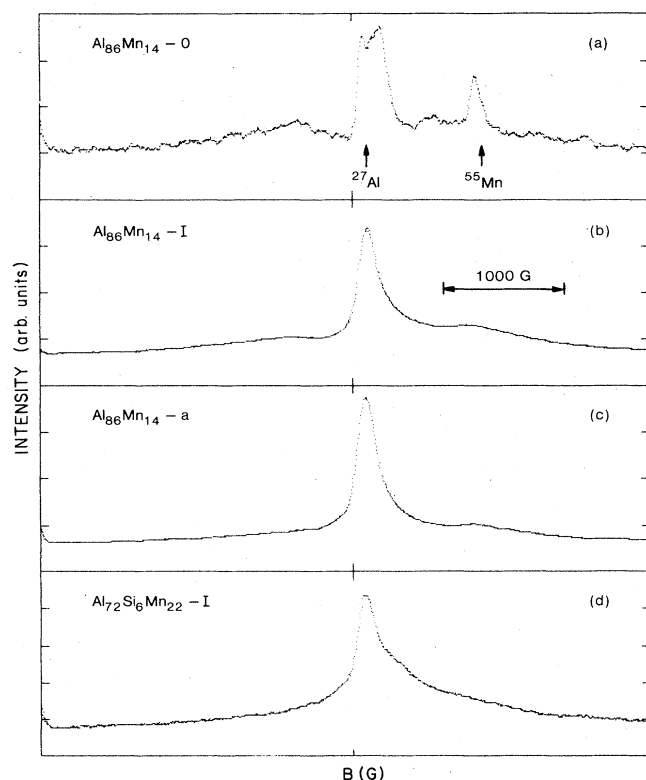


FIG. 1. Spin-echo spectra at 4.2 K measured at fixed frequency 18.3 MHz: (a) $\text{Al}_{86}\text{Mn}_{14}$ annealed to equilibrium crystalline phase, (b) icosahedral quasicrystal $\text{Al}_{86}\text{Mn}_{14}\text{-I}$, (c) amorphous form $\text{Al}_{86}\text{Mn}_{14}\text{-a}$, (d) icosahedral quasicrystal $\text{Al}_{72}\text{Si}_6\text{Mn}_{22}\text{-I}$. Arrows indicate reference positions of ^{27}Al and ^{55}Mn resonances ($\gamma^{27}\text{Al} = 1.1094 \text{ kHz/G}$ and $\gamma^{55}\text{Mn} = 1.0500 \text{ kHz/G}$).

order quadrupole splitting. The separation of the high-field peak, attributed to ^{55}Mn , exhibits the expected linearity with the frequency.

In Fig. 3 we show a separation of the ^{27}Al and ^{55}Mn lines for $\text{Al}_{86}\text{Mn}_{14}\text{-I}$ obtained by reflecting the observed spectrum about the center of the narrow ^{27}Al line and subtracting the reflected spectrum from the total at high field. The result consists of a symmetrized ^{27}Al quadrupole pattern and a single broad ^{55}Mn line. We neglect in this analysis the small asymmetry of the ^{27}Al central peak. A similar treatment of the spectrum for $\text{Al}_{86}\text{Mn}_{14}\text{-a}$ yields a ^{55}Mn resonance at the same position with essentially the same width.

The first-order electric quadrupole spectrum depends on the magnitude and symmetry of the local EFG V_{ij} . The EFG tensor is completely determined by two parameters defined in its principal axis coordinate frame: the maximum component V_{zz} and the asymmetry parameter $\eta = (V_{xx} - V_{yy})/V_{zz}$ with $0 \leq \eta \leq 1$. For ^{27}Al and ^{55}Mn (spin $I = \frac{5}{2}$) the splitting frequency is $\nu_Q = \frac{3}{20} V_{zz} Q/h$, where Q is the nuclear quadrupole moment. The mean value $\bar{\nu}_Q$ determines the overall breadth of the spectrum, while the shape of the powder pattern depends on the asymmetry η .

The quadrupole pattern for $\text{Al}_{86}\text{Mn}_{14}\text{-I}$ is not consistent with the powder pattern shapes expected¹⁰ for single values of ν_Q and η at the Al sites, but instead implies the presence

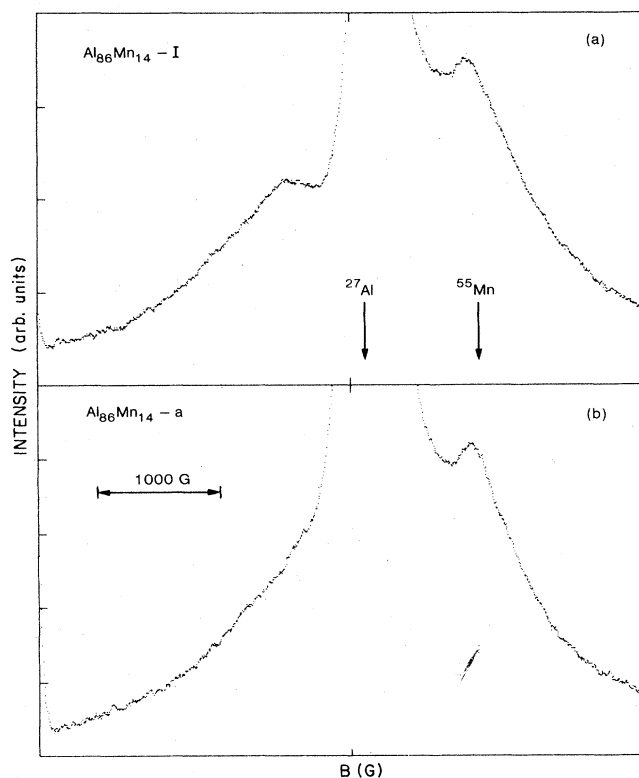


FIG. 2. Broad spectra comparison of (a) icosahedral phase $\text{Al}_{86}\text{Mn}_{14}\text{-I}$ and (b) amorphous form $\text{Al}_{86}\text{Mn}_{14}\text{-a}$.

of distributions in these quantities. We have established roughly the ranges of these distributions by means of numerical simulation. A calculated spectrum is compared with the data in Fig. 3. The simulation shown is an equally weighted superposition of six quadrupole patterns for η values uniformly distributed over the range $0.1 \leq \eta \leq 0.6$. Each pattern was broadened by a Gaussian distribution of ν_Q values with second moment $\Delta\nu_Q/\bar{\nu}_Q = 0.3$ and $\bar{\nu}_Q = 2.1 \text{ MHz}$. A Lorentzian distribution represents the central transition. Given the large number of parameters and dearth of distinct spectral features, we caution that the high quality of the fit cannot be taken as evidence that the distributions of ν_Q and η are correct in detail. Nor do we claim any special significance for the use of six η values. A larger or slightly smaller number works as well. We did find, however, that the fit was seriously degraded by significant increases or decreases in $\Delta\nu_Q$ [$\delta(\Delta\nu_Q/\bar{\nu}_Q) \geq 0.1$], and inclusion of higher η values did not permit even qualitative reproduction of the observed powder pattern. Thus we can conclude that the majority of Al sites in the icosahedral phase have low to medium asymmetry and that the spread in ν_Q values is of the order of $\pm 30\%$.

We can now ask how the ranges of ν_Q and η values must be changed to explain the spectrum obtained for amorphous $\text{Al}_{86}\text{Mn}_{14}$. We found that inclusion of η values up to $\eta = 0.9$ together with a modest increase in $\Delta\nu_Q$ ($\Delta\nu_Q/\bar{\nu}_Q = 0.4$) is sufficient to eliminate the shoulders seen in the spectrum of the icosahedral phase and produce a simulated line shape in agreement with that observed for

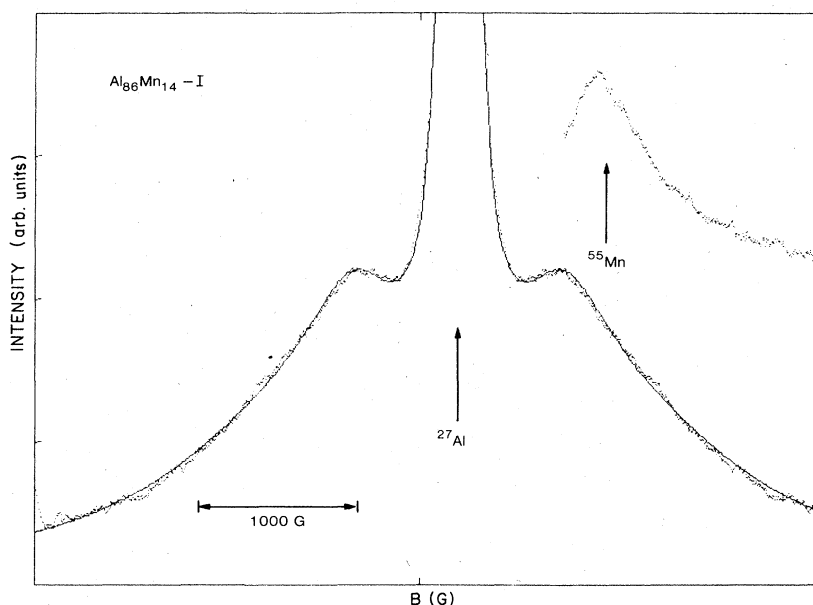


FIG. 3. Spectrum of icosahedral phase $\text{Al}_{86}\text{Mn}_{14}\text{-I}$ decomposed to display ^{27}Al electric quadrupole splitting pattern and ^{55}Mn resonance. Solid line represents numerical line-shape simulation described in text.

$\text{Al}_{86}\text{Mn}_{14}\text{-a}$ [Fig. 2(b)]. We could not obtain a successful fit by broadening only the distribution in ν_Q . Thus the main distinction between the amorphous and icosahedral forms of $\text{Al}_{86}\text{Mn}_{14}$ is the exclusion of high asymmetry in the EFG at the Al sites in $\text{Al}_{86}\text{Mn}_{14}\text{-I}$. In agreement with recent Mössbauer studies,⁷ we find no significant difference between the relatively broad EFG distributions at the Mn sites in the two forms. We note, in particular, that the ^{55}Mn resonance in the icosahedral phase does not exhibit the quadrupolar structure to be expected if there were only two types of site in the quasicrystal.¹¹ Although we have not

analyzed in detail the spectrum of the ternary alloy $\text{Al}_{72}\text{Si}_6\text{Mn}_{22}$, it is evident from the lack of resolved structure [Fig. 1(d)] that the EFG distributions at both Al and Mn sites are broader than in either the icosahedral or amorphous forms of the binary $\text{Al}_{86}\text{Mn}_{14}$.

The authors wish to express their appreciation to G. F. Brennert who took part in the preparation of the NMR experiments and to R. J. Felder for his assistance in preparing the sputtered amorphous sample.

¹D. Schechtman, I. Blech, D. Gratias, and J. W. Cahn, *Phys. Rev. Lett.* **53**, 1951 (1984).

²C. H. Chen and H. S. Chen, *Phys. Rev. Lett.* (to be published).

³For a recent review, see D. R. Nelson and B. I. Halperin, *Science* **229**, 233 (1985).

⁴D. Levine and P. J. Steinhardt, *Phys. Rev. Lett.* **53**, 2477 (1984).

⁵V. Elser, *Phys. Rev. B* **32**, 4892 (1985).

⁶M. Duneau and A. Katz, *Phys. Rev. Lett.* **54**, 2688 (1985).

⁷M. Eibschutz, H. S. Chen, and J. J. Hauser (unpublished).

⁸H. S. Chen, C. H. Chen, A. Inoue, and J. T. Krause, *Phys. Rev. B* **32**, 1940 (1985).

⁹H. S. Chen and C. H. Chen, *Phys. Rev. B* (to be published).

¹⁰See, for example, G. C. Carter, L. H. Bennett, and D. J. Kahan, *Metallic Shifts in NMR* (Pergamon, Oxford, 1977), Pt. I, p. 71.

¹¹L. J. Swartzendruber, D. Schechtman, L. Bendersky, and J. W. Cahn, *Phys. Rev. B* **32**, 1383 (1985).